Contact Dynamic Modeling of a Liquid Droplet Between Two Approaching Porous Materials

Homayun K. Navaz, Ali Zand, Theresa Atkinson, and Albert Nowakowski
Kettering University, Flint, MI 48504

Amir Gat
California Institute of Technology, Pasadena, CA 91125

Sari Paikoff
Defense Threat Reduction Agency (DTRA), Fort Belvoir, VA 22060

DOI 10.1002/aic.14387
Published online February 26, 2014 in Wiley Online Library (wileyonlinelibrary.com)

A computational fluid dynamics model based on a finite difference solution to mass and momentum conservation equations (Navier–Stokes equations) for a liquid droplet transport between two porous or nonporous contacting surfaces (CSs) is developed. The CS dynamic (equation of motion) and the spread of the incompressible liquid available on the primary surface for transfer are coupled with the Navier–Stokes equations. The topologies of the spread dynamic between and inside both surfaces (primary and CSs) are compared with experimental data. The amount of mass being transferred into the CS, predicted by the model, is also compared to the experimental measurements. The impact of the initial velocity on the spread topology and mass transfer into the pores is addressed. © 2014 American Institute of Chemical Engineers *AIChE J*, 60: 2346–2353, 2014
Keywords: computational fluid dynamics, porous media, fluid mechanics, mass transfer

Introduction

The spread of liquid toxic chemical agents in the environment poses a great threat to humans. One of the ways that these chemicals can pose a threat to lives is through direct contact with clothes or skin. This threat becomes more serious if their release takes place with malicious intentions. Under such circumstances, the first responders have to make quick but difficult decisions that have direct impacts on lives. It is preferred that these decisions be based on scientific analysis and data. In general, these exposures can occur by inhalation, ingestion, and direct contact. Low volatile chemicals have the tendency to be more of a threat through direct contact in their liquid form with surfaces like skin and equipment. Furthermore, due to their persistency and low evaporation rate, they pose more of a threat to warfighters and first responders as they move through an affected area. Therefore, the dynamics of liquid transport onto warfighters' clothing and equipment creates a hazardous scenario. The inspiration hazard that is more specific to "higher" volatile chemicals occurs when a chemical has evaporated. The evaporation can occur when droplets of a chemical are visible on a surface and also can take place when a droplet sinks into a porous environmental substrate and will gradually become available at the surface as the liquid slowly evaporates within the pores. Generally, warfare chemical agents or pesticides are disposed in droplet form, and upon their absorption into a porous substrate continue to pose a contact hazard at the surface.

The fate of a wetting liquid droplet deposited onto a porous medium surface determines the amount of mass available for the transfer into a secondary (or contacting) surface. Focusing solely on the momentum transport mechanism, the flow of a sessile liquid generally takes place in two directions, lateral (spread on the surface of the porous material) and vertical (infiltration into the porous material). To calculate the time, it takes for the droplet to penetrate into a porous medium, Denesuk et al. have used both constant and decreasing droplet base radii.[1] A detailed study of how the droplet base radius changes for complete and partially wetting liquids has been carried out,[2,3] where they found a unique dependence of base radius on time. Holman et al. have shown that the extent of the surface flow depends on the permeability of the porous material.[4] For low permeable materials, the surface tension can be sufficiently high to prevent the surface flow. Evidence indicates the surface spread is coupled with the infiltration flow into the porous medium. In all of these studies, the wetted region is fully saturated with a clearly defined wetting front. However, Popovich et al. have shown that the liquid/porous medium can create regions with saturations less than unity depending on their wetting characteristics.[5] Several parameters affect the amount/concentration of transferred agent. These include porosity, capillary pressure, viscosity, surface tension, density, and philicity. This process becomes more complex if phase change, chemical reaction, and adsorption also present

Correspondence concerning this article should be addressed to A. Gat at amirgat@caltech.edu.

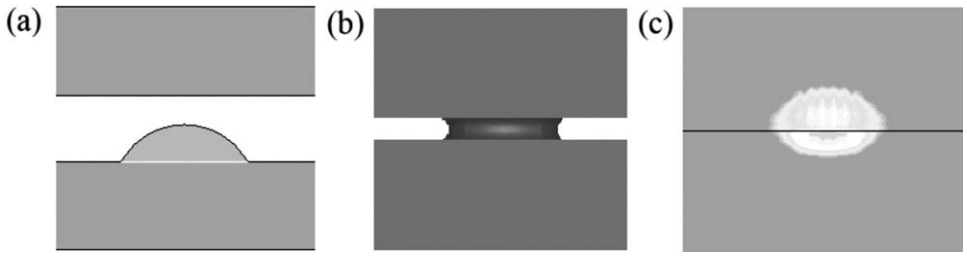

Figure 1. Schematics of precontact, contact, and postcontact phases: (a) precontact, (b) contact with liquid bridge, (c) contact.

themselves as source or sink terms. Depending on the relative magnitudes of these processes rates, a different temporal and spatial distribution of the initial liquid phase can be expected in the domain under consideration.[6–8] The spread of a liquid droplet on a porous surface and its infiltration into porous medium starts immediately after it is deposited on the surface, due to the capillary action caused by capillary pressure and saturation gradients. The liquid infiltration continues even when there is no free liquid left on the porous medium surface inducing the multiphase flow to emerge. This process causes the liquid phase to still be available at the surface (especially after an equilibrium has been reached) with saturation less than unity and still pose a direct contact hazard. This is more of a threat if the contacting surface (CS) demonstrates more hydrophobic properties, where more chemical is available on the surface. A good example is moisturizing creams that can immediately penetrate skin after contact.

The initial velocity (a result of exerted force) during contact will determine the extent of the wetted footprint which in part will determine the available surface area for any mass transfer during contact. As the size of the imprint increases, more area will be contaminated and pose an increased risk due to the availability of a larger contact hazard area. There is also a precontacting period that specifies the amount of liquid chemical that is available for transfer to a CS, if the liquid contaminant is initially residing on a porous substrate.

There are numerous experimental studies in the literature that examine the absorption of chemicals into skin or some other porous materials. A recent review article by Ngo et al. is a comprehensive discussion of the available experimental data in this research field.[9] There are also some models available that are based on linear regression performed on experimental data. The approximate analytical models that determine the dynamic of the liquid bridge between two surfaces are discussed by Gat et al.[10] Extensive studies by Bijeljic, Markicevic, and Navaz study the spread of sessile droplets within porous environmental substrates.[11–13] D'Onofrio et al. have also presented the validation of their capillary network model with experimental data for HD and VX nerve agents.[14] Navaz et al. have presented a methodology to derive the capillary pressure function for the spread at a sessile droplet into a porous material.[15] They have demonstrated that a simple experimental measurement can determine the capillary pressure function for any droplet size for a given liquid and substrate. The use of finite difference method for solving the combined porous medium flow and sessile droplet dynamics was introduced by Navaz et al.[15] Masoodi et al. have also developed a numerical algorithm for the transport of liquids in porous material on a stationary elements (or mesh).[16] This work is the extension of our three-dimensional (3-D) finite difference algorithm for the transport of liquids in porous materials that was published in 2008. The adaptive meshing with a second surface motion is added to our previous code to simulate the contact and wicking processes. It should be noted that the focus of this work is to (a) develop a general-purpose computational model that can simulate all the possible scenarios for precontact and contact processes and (b) to present such an algorithm for solving the transfer, spread, and transport of a preexisting liquid droplet situated on a porous (or nonporous) substrate into a porous CS. This code is meant to become a workhorse for the contact hazard where the amount of mass transported to a surface is of primary interest. The topology of the interface between the wetting and nonwetting fluids can be changed and studied further according to the formulation in Appendix, in the context of the total amount of mass transfer into the CS which provides valuable information for toxicologists. The contact time is usually much less than the entire capillary transport and it is assumed that the shape of this interface will not have a significant effect on the amount of mass being transferred to either medium.

Model

The contact of two approaching surfaces can be divided into three steps, schematically shown in Figure 1. The first step is the precontact phase where a sessile droplet is residing on a nonporous or porous surface referred to as the primary surface (PS). We refer to this liquid as the free volume liquid ($\forall_{\text{free}}$). The volume of liquid that is transported into the PS through the surface is ($\forall_{\text{PS}}$). The capillary transport of the liquid droplet into the PS will take place until the time of contact with the free volume liquid that may be present on the PS. The availability of this liquid depends on the transport properties of the PS and the time interval for the contact. If $\forall_{\text{free}} > 0$, the liquid droplet will be sandwiched between the two surfaces creating a liquid bridge. However, if there is no free liquid left on the surface at the time of contact, the transfer from the PS to the CS will take place when the two surfaces touch. Upon a perfect contact, the value of saturation and its normal gradient in both media (zones) are assumed to be equal. This is usually referred to as "perfect contact" boundary condition. Similar boundary conditions can also be imposed on the CSs to obtain a numerical solution. When $\forall_{\text{free}} > 0$, the liquid bridge is assumed to have the shape of a hyperboloid with a decreasing height. The contact angle of this hyperboloid and the surfaces can be found through experiments. The remaining volume of the liquid bridge is calculated each time step after its capillary transport into the porous media. The separating

distance is also calculated for each time step. By knowing the mass of the liquid bridge and its height, the CS area (assumed to be circular) is updated in each time step. The rate of the radius increase will determine the spread rate.

The continuum formulation for the transport of a liquid sessile droplet into a porous medium is given by Navaz et al.[15] The equation of motion is added to the set and the coupled equations are given as

$$\frac{\partial(\phi\rho_{\ell i}s_{\ell i})}{\partial t}+\nabla\bullet\left(\phi\rho_{\ell i}s_{\ell i}\vec{V}_{\ell i}\right)=0$$

$$\vec{V}_{\ell i}=-\frac{Kk_{\ell i}}{\mu_\ell}(\nabla P_{\ell i}-\rho_{\ell i}gs_{\ell i}),\quad P_{\ell i}=P-P_{ci}\ \text{(Capillary)},\quad K=\text{Saturation permeability},\quad \mu=\text{Viscosity}$$

$$\rho_{\ell i}=\text{Density of liquid phase constituent }''i'',\quad s_{\ell i}=\text{Saturation of liquid constituent }''i'' \tag{1}$$

$$\text{Equation of Motion}:\ y=V_ot+y_o$$

$$y=\text{Coordinate system (Vertical)}\quad V_o=\text{Initial Velocity}\quad y_o=\text{Initial space between the two surfaces}$$

For this work, we are focusing on the process of contact and will postpone the multispecies solution to future analysis. Furthermore, all the source terms defining the adsorption, evaporation, and chemical reaction are also dropped for now. Equations 1 were transformed into the computational domain [$\xi=\xi(x,y,z)$, $\eta=\eta(x,y,z)$, $\zeta=\zeta(x,y,z)$] and marched in time to obtain the saturation function. The explicit fourth-order Runge–Kutta scheme was used to solve for the saturation.[15] The motion of the liquid bridge is terminated when both surfaces come into contact and the saturation at the contact boundary falls below unity due to absorption process into the porous media. It should be noted that we have assumed perfect contact between the two surfaces, that is, the following relationships for the saturation hold

$$s_{\text{Upper boundary of the lower surface}}=s_{\text{Lower boundary of the upper surface}}$$

$$\left(\frac{\partial s}{\partial n}\right)_{\text{Upper boundary of the lower surface}}=\left(\frac{\partial s}{\partial n}\right)_{\text{Lower boundary of the upper surface}} \tag{2}$$

where n is the normal direction to the surface.

The transport of mass across the boundary continues for some time before equilibrium is reached. Figure 2 shows that the mass transfer across the boundary continues for a few hours if the liquid does not evaporate after the contact due to capillary and gravity effects. A very small amount of mass is transferred from the lower medium to the upper medium through the interface in longer period of time due to the capillary pressure.

The continuity and momentum equations are numerically integrated in time to find the distribution of liquid droplet inside the pores. At the boundary between the droplet and the porous substrate, the saturation is unity ($s_\ell=1$) and the capillary pressure is enhanced by the local hydrostatic pressure (based on local height, h^* in Figure 1a) as: $P_\ell=P-P_{ci}+\rho_\ell gh^*$. Mass is being transported into porous medium according to $(\rho_\ell\tilde{v}\varphi)/J$; where J is the Jacobian for the transformation and $\tilde{v}$is the contravariant vertical velocity given by: $\tilde{v}=\eta_x u+\eta_y v+\eta_z w$ with u, v, w being the three components of the velocity and η_x, η_y, η_z being the metrics for the transformation. The mass transfer is calculated in each time step and the instantaneous remaining mass yields the liquid bridge volume. The volume of the hyperboloid was derived by deducting the volume of a "partial" torus from a cylinder with the base radius of r (liquid footprint) and height h using the Pappus second theorem (see Appendix).

The equation correlating instantaneous $r(t)$ and $h(t)$ with the liquid volume $\forall_{\text{Liquid Bridge}}(t)$ can be obtained as

$$r^2(t)-\frac{h(t)G(\beta)}{4\cos^2\beta}r(t)-\frac{h^2(t)G(\beta)\tan\beta}{8\cos^2\beta}+\frac{h^2(t)}{6}-\frac{\forall_{\text{Liquid Bridge}}}{\pi h(t)}=0 \tag{3}$$

$$G(\beta)=\pi-2\beta-\sin(\pi-2\beta)$$

β is the contact angle between the surface and the liquid bridge. The droplet base radius (footprint), $r(t)$ is calculated from the above equation. Both domains (or media) are remeshed and adapted to the new footprint of the liquid bridge. The remeshing is done after each time step. Figure 3 depicts two top view snapshots of the adaptive mesh configurations and Figure 4 displays the liquid bridge configurations before the contact, during the spread, and finally after the gap between the two surfaces is closed. The last snapshot (4a) also signifies the fact that the saturation at the interface

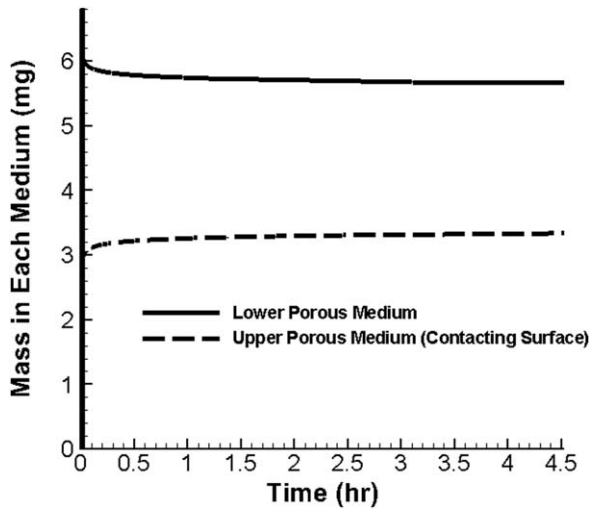

Figure 2. 9-μL VX sessile droplet on sand (Φ = 0.35) mass transport into another porous medium (Φ = 0.35).

The largest amount of mass is transferred to the CS during the first few minutes. The transfer of mass significantly slows down after the contact and asymptotically reaches an equilibrium conditions after about 5 h.

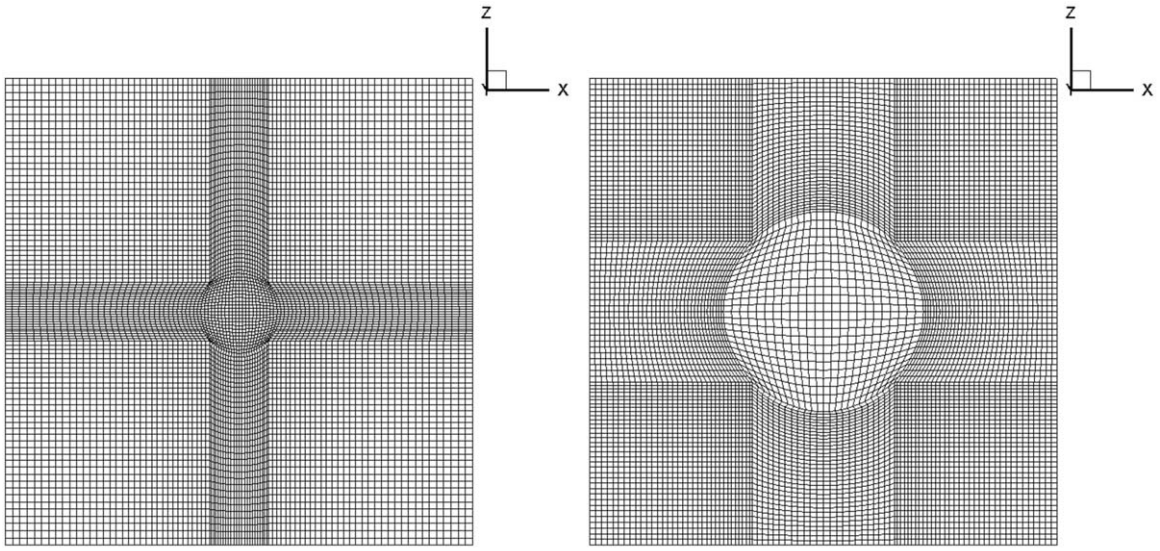

Figure 3. (a) Top view of the adaptive mesh when liquid bridge still expanding, when Eq. 33 is valid, and (b) the final configuration of the mesh when Eq. 44 is valid and also as time $\rightarrow \propto$ for nonevaporating liquids (final grid is stationary).

will not stay at unity and will become less than 1 as the capillary transport continues.

As the gap between the two surfaces is closing, the height will reduce. At the same time, the liquid is absorbed into the porous media. Therefore, $h(t)$ and $\forall_{\text{Liquid Bridge}}(t)$ are updated in each time step and the spread rate $dr(t)/dt$ can be obtained. Note that the $h(t)$ is determined by the equation of motion during this phase. Furthermore, when the height of the liquid bridge becomes less than a threshold, the spread is stopped. This threshold is a function of surface roughness and viscosity of the fluid, and can also be determined experimentally. At this point, the radius of the footprint remains constant and the absorption is driven solely by capillary pressure causing a reduction in $h(t)$. This value of $h(t)$ can be calculated by solving the above equation again with the "final" liquid footprint radius. This equation is given as

$$\left(\frac{\pi}{6}-\frac{\pi G(\beta)\tan\beta}{8\cos^2\beta}\right)h^3(t)-\frac{\pi r(t)G(\beta)}{4\cos^2\beta}h^2(t)+\pi r^2(t)h(t)-\forall_{\text{Liquid Bridge}}=0 \quad (4)$$

This will be a cubic equation in $h(t)$. As the absorption into the porous media occurs, the volume of the droplet is updated and the new $h(t)$ is calculated. The detailed derivations of these equations are outlined in Appendix.

It should be noted that the time required for the topology of a sessile droplet (Figure 1a) to change to a liquid bridge (Figure 1b) is estimated to have a magnitude of $O\left(r_o^2\mu/\sigma z_o\right)$ where r_o and z_o are characteristic lengths in vertical (direction of motion) and radial (direction of spread) directions, respectively. μ is the viscosity and σ is the surface tension. The momentum equation in radial direction can be used to conclude this.[17] This is negligible compared to the magnitude of time required for liquid to penetrate the porous medium, that is, $O\left(r_o^2\mu/\sigma\sqrt{k}\right)$ with K being the permeability. Therefore, it is acceptable to ignore the time required for the topology change from sessile droplet to a liquid bridge and define the liquid bridge topology by knowing the volume of the droplet during the contact and the distance between the two surfaces. The liquid bridge footprint can be calculated according to Eq. 2.

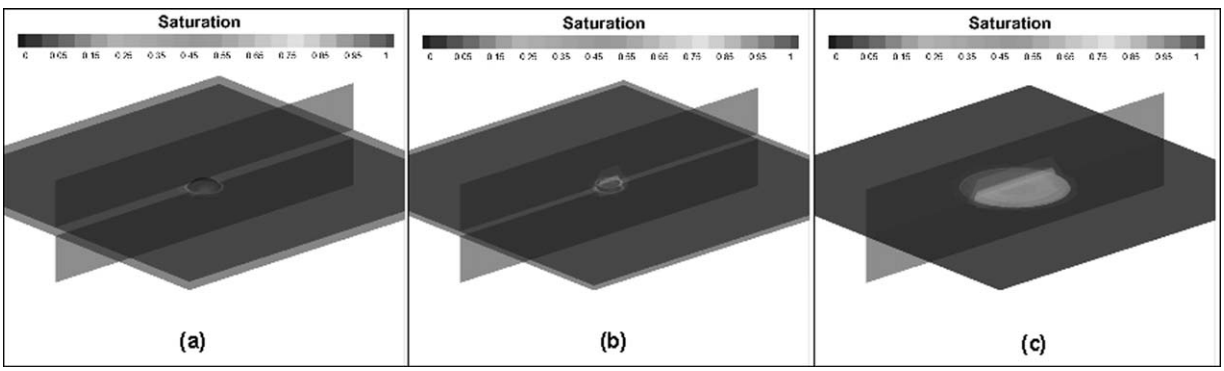

Figure 4. (a) Precontact configuration when the droplet is being absorbed into the lower surface.

The mesh is stationary and mass being transported through a constant circular area, (b) contact configuration when the liquid bridge is formed and the footprint radius is reduced and expanded after that if absorption takes place slower than the spread. Adaptive meshing is required for this stage, and (3) postcontact, when the two surfaces are in perfect contact and the saturation falls below unity at the interface due to capillary transport.

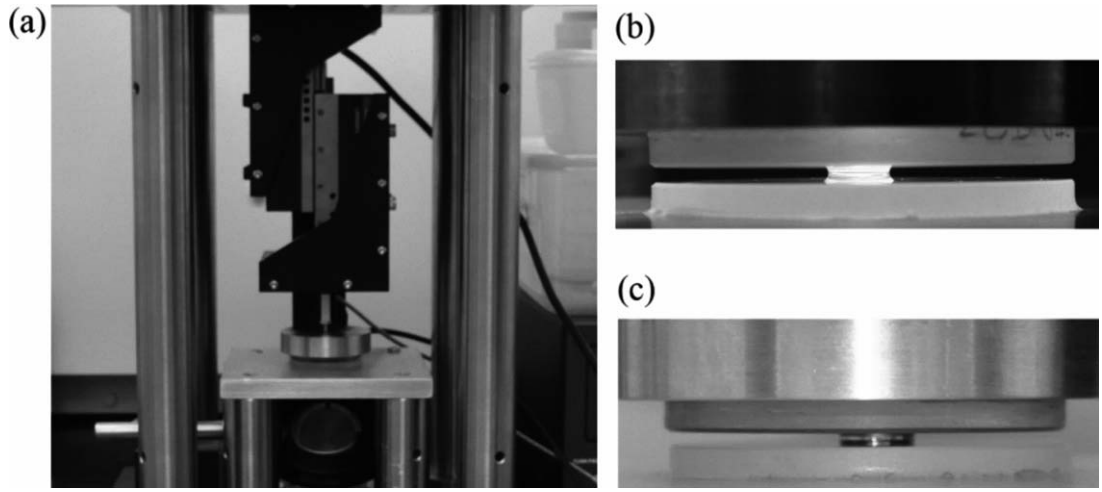

Figure 5. (a) The experimental setup: two fused-silica plates connected by (b) a DI water liquid bridge (c) and mercury liquid bridge.

Results and Discussion

The experimental setup consists of a linear stage actuator (Thorlabs™ LNR50SEK1) controlling the distance between two parallel plates, a load cell (Interface™ MB-LBF5) measuring the force acting on the solid body, and two optical windows (Newport™ 20BW40-30) used as the upper and lower plates. A feedback control loop was created, connecting the load-cell force input, the actuator position, and speed inputs and outputting the upper plate acceleration and speed. The feedback was programmed to simulate a freely moving solid body with a given mass, m_1, reacting to external forces and the force applied by the liquid bridge connected to a solid body with mass $m_2 \rightarrow \infty$. The plates are cleaned before each experiment by Acetone, Isopropanol, and Nitrogen gas. The advancing and receding wetting angles were estimated from quasistatic force measurements.[18] Figure 5 shows the experimental setup. This is a new approach based on continuum formulation. It is intended to be widely used by government and industry. Therefore, it is necessary to perform extensive validation of the code.

In the first test case, a 20-μL glycerin droplet was deposited on play sand (porosity = 35%) and a cloth was brought into contact with glycerin. The initial distance was 11 cm, and the approach speed of the CS was 35 cm/s. The amount of mass absorbed into the cloth was recorded and compared to the model prediction in Figure 6. The porosity of both surfaces in this case is fairly high and we do not expect much of a spread. That is to say that the amount of spread and footprint of the liquid is a function of the porosity and permeability, the more mass being absorbed into the CS, the less is available to be spread.

A second experiment was conducted by putting a 20-μL glycerin droplet on kitchen tile with a porosity of 24%. A wafer was made in our laboratory from filter paper pulp with a porosity of 70% to serve as the secondary surface. Five separate experiments (three repetitions for each experiment) were conducted. The two surfaces were brought into contact after 1, 10, 20, 30, and 40 min, in which a different amount of glycerin on the surface of the tile was available for transfer into the filter paper wafer. The exerted force was 1 N for all cases and all experiments started with an initial 2.5-cm

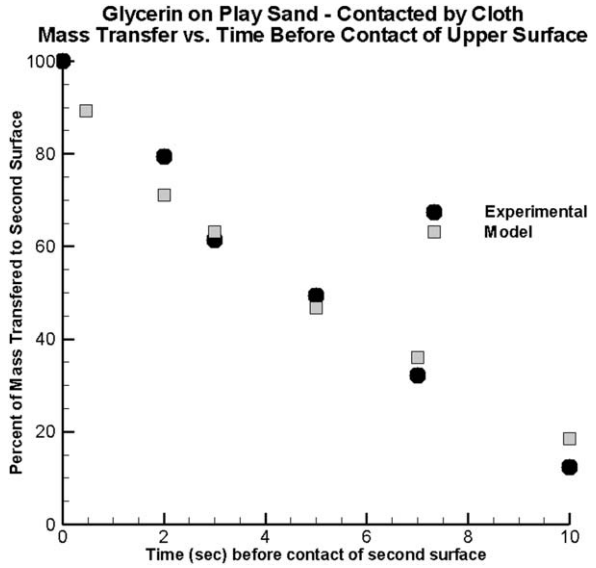

Figure 6. Mass transfer of glycerin initially saturated on sand to cloth by contact as a function of time elapsed after the contact.

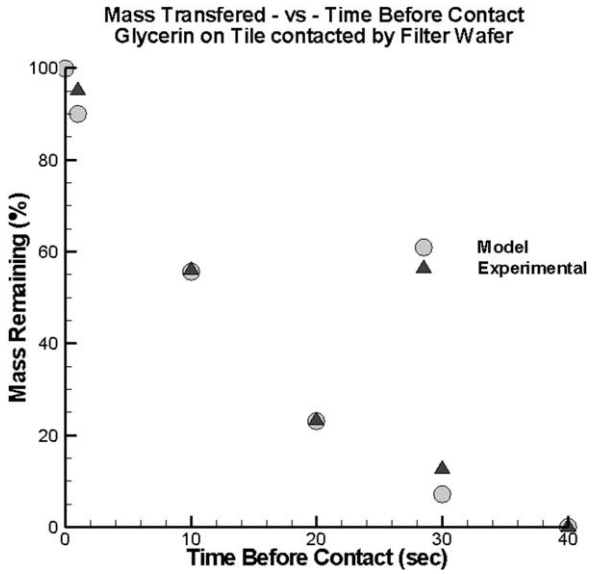

Figure 7. Mass transferred to CS as a function of time elapsed after the contact.

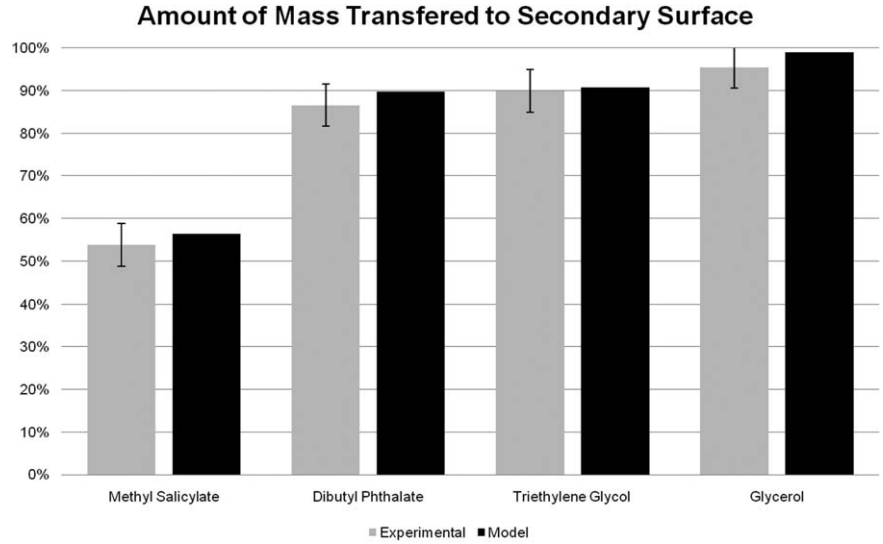

Figure 8. Comparison of model prediction with experimental data for four different chemicals.

Chemicals were placed on glass slides and were contacted by a second surface of filter paper.

distance between the two surfaces. The amount of transferred glycerin in the secondary surface (wafer) was measured and is compared with the model predictions in Figure 7. These comparisons indicate that the model is fairly accurate in predicting the amount of mass being absorbed into a contacting porous surface.

In another set of validation tests, glass and filter paper were selected as the primary and secondary surfaces, respectively. The two surfaces were brought into contact, and the amount of mass absorbed into the filter paper was measured and compared with the computational model. The initial gap and approach velocity between the two surfaces were similar to the previous test case. These tests were conducted with four different chemicals and the results are depicted in Figure 8. The comparison shows that the model is robust as the physiochemical properties are altered. The presented cases indicate that the model is accurate in predicting the amount of mass that is absorbed when a contact occurs. This is operationally relevant and useful information to assess the amount of threat or contamination.

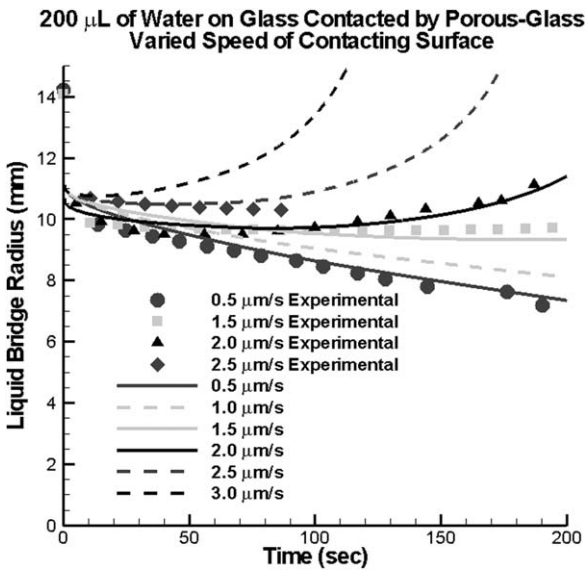

Figure 9. 200-μL of water on glass contacted by porous glass.

The approach velocities of 0.5, 1.5, 2.0, and 2.5 μm/s are compared with the model. Two additional velocities of 1.0 and 3.0 μm/s are also modeled. For lower velocities, the absorption into porous glass is at a faster pace than the spread speed causing a continuous reduction in radius in time. As the approach velocity increases, the spread will proceed at a faster pace than the absorption causing a continuous increase of radius in time. It appears that at velocity of 1.5 μm/s both processes take place at the same "speed."

However, another test case was considered to compare the spread rate in radial direction with absorption or transfer rate into a porous medium. The experimental setup consists of the same linear stage actuator used for the previous experiments. 200-μL deionized (DI) water was used as a sessile droplet deposited onto a fused silica optical window, as the impermeable surface, and a porous glass (VykorTM7930) was used as the permeable CS. The physical properties of water are $\mu=0.001\,\mathrm{Pa.s}$, $\rho=1000\,\mathrm{kg/m^3}$, $\sigma=0.072\,\mathrm{N/m}$. The porous glass has the porosity of 28% with permeability of 2.08×10^{-19} $\mathrm{m^2/s}$. The surfaces were brought into contact with velocities of 0.5, 1.5, 2.0, and 2.5 μm/s, and the liquid bridge radius was measured and calculated by the model as a function of time. The results of this study are shown in Figure 9. In all cases, there is an initial decrease in the radius that is due to the topology transfer from a sessile droplet to a hyperboloid topology. For smaller approach velocities, the absorption into the porous medium proceeds faster than the spreading causing a steady reduction in the footprint radius in time. It appears that the radius does not change significantly in time after the initial adjustment for the approach velocity of 1.5 μm/s demonstrating that the amount of mass absorbed into the porous medium is at a value that does not allow further spread of the liquid bridge. Basically, there is not enough mass left to be spread. We have also modeled two additional approach velocities of 1.0 and 3.0 μm/s to demonstrate the consistency of the results. It is seen that as the velocity of approach increases, the absorption process is dominated by the liquid bridge motion, causing an increase in the footprint radius in time. It should be noted that although more

surface area becomes available for the mass transport during a fast spread, it is not enough for the capillarity to be a dominant process.

Concluding Remarks

A computer model for the transfer and radial spread of a sessile liquid droplet initially resting on a porous or nonporous surface and becoming a liquid bridge upon the contact with another surface was developed. The model solves the transport equations for capillary flow in 3-D based on finite-difference discretization of the governing equations with Runge–Kutta fourth-order algorithm. The liquid bridge shape is assumed to be a hyperboloid and its radius is determined from the liquid volume and the distance between the two surfaces. The model can accurately predict the spread and transfer of chemicals into porous surfaces upon contact. This information is necessary to assess and mitigate the extent of a threat posed by chemical agents. This study focused on motion in the vertical direction perpendicular to the planes of parallel surfaces. However, the motion in the tangential direction can also occur enhancing the amount of mass transfer to the porous CS. This will be addressed in our future research.

Acknowledgments

This research was supported by the Defense Threat Reduction Agency (DTRA) under the contract HDTRA1–10-C-0064. The authors thank the agency for their continued support and vision in the CHEM/BIO Defense area.

Literature Cited

1. Denesuk M, Smith GL, Zelinski BJJ, Kreidl NJ, Uhlmann DR. Capillary penetration of liquid droplets into porous materials. *J Colloid Interface Sci*. 1993;158:114–120.
2. Starov VM, Kostvintsev SR, Sobolev VD, Velarde MG, Zhdanov SA. Spreading of liquid drops over dry porous layers: complete wetting case. *J Colloid Interface Sci*. 2002;252:397–408.
3. Starov VM. Surfactant solutions and porous substrates: spreading and imbibitions. *Adv Colloid Interface Sci*. 2004;111:3–27.
4. Holman RK, Cima MJ, Uhland SA, Sachs E. Spreading and infiltration of inkjet-printed polymer solution droplets on a porous substrate. *J Colloid Interface Sci*. 2002;249:432–440.
5. Popovich LL, Feke DL, Manas-Zloczower I. Influence of physical and interfacial characteristics on the wetting and spreading of fluids on powders. *Powder Technol*. 1999;104:68–74.
6. Nikolopoulos N, Theodorakakos A, Bergeles G. A numerical investigation of the evaporation process of a liquid droplet impinging onto a hot substrate. *Int J Heat Mass Transf*. 2007; 50:303–319.
7. Zadražil A, Stepanek F, Matar OK. Droplet spreading, imbibition and solidification on porous media. *J Fluid Mech*. 2006;562: 1–33.
8. Reis NC Jr, Griffiths RF, Mantle MD, Gladden LF. Investigation of the evaporation of embedded liquid droplets from porous surfaces using magnetic resonance imaging. *Int J Heat Mass Transf*. 2003;46: 1279–1292.
9. Ngo MA, O'Malley M, Maibach HIJ. *Appl Toxicol*. 2010.
10. Gat A, Navaz HK, Gharib M. Dynamics of solid bodies connected by shallow liquid bridges. *Phys Fluids*. 2011;23.
11. Bijeljic B, Markicevic B, Navaz HK. Capillary climb dynamics in the limits of prevailing capillary and gravity force. *Phys Rev E*. 2011;83:Art. No. 056310.
12. Markicevic B, Navaz HK. Primary and secondary infiltration of wetting droplet into porous medium. *Transp Porous Media*. 2010;85: 953–974.
13. Markicevic B, D'Onofrio TG, Navaz HK. On spread extent of sessile droplet into porous medium: numerical solution and comparisons with experiments. *Phys Fluids*. 2010;22:Art. No. 012103.
14. D'Onofrio TG, Mantooth BA, Sumpter KB, Markicevic B, Navaz HK. Experimental and numerical study of spread and sorption of VX sessile droplet into medium grain-size sand. *Langmuir*. 2010;26: 3317–3322.
15. Navaz HK, Markicevic B, Zand AR, Sikorski Y, Chan E, D'Onofrio TG. Sessile droplet spread into porous substrates - determination of capillary pressure using a continuum approach. *J Colloid Interface Sci*. 2008;325:440–446.
16. Masoodi R, Tan H, Pillia KM. Darcy's law–based numerical simulation for modeling 3D liquid absorption into porous wicks. *AIChE J*. 2011;57:1132–1143.
17. Gat A, Navaz HK, Gharib M. Wicking of a liquid bridge connected to a moving porous surface. *J Fluid Mech*. 2012;703:315–325.
18. de Souza EJ, Gao L, McCarthy TJ, Arzt E, Crosby AJ. Effect of contact angle hysteresis on the measurement of capillary forces. *Langmuir*. 2008;24:1391–1396.

Appendix

Consider the following configuration that displays an arc revolving around the C-C′ axis. The goal is to find the volume of this body of revolution. If point A is the centroid of the surface engulfed by the arc FMG, the volume of the partial torus shaped resulting from this revolution according to Pappus Centroid Theorem is shown in Figure A1.

Volume of the partial torus $= V_{pt} = 2\pi A\overline{OA}$ where A is the area of the arc. Then, the volume of the liquid between the two surfaces will be

$V_{Liq} = \pi r^2(t)h - V_{pt}$ where t represents the time. Note that both the footprint radius and the liquid bridge height both are functions of time and are calculated in each time step. If $\hat{\theta}$=GBF then

$$AB = \frac{4R(t)\sin^3\frac{\theta}{2}}{3(\theta - \sin\theta)}$$

$$R(t) = \frac{h(t)}{2\cos\beta}$$

$$V_{Liq} = \pi r^2(t)h(t) - 2\pi\left[\frac{R^2(t)}{2}(\theta - \sin\theta)\right]\left[r(t) + \frac{h(t)}{2}\tan\beta - AB\right] \tag{A1}$$

The instantaneous footprint radius can be obtained from this equation by knowing the volume of the liquid bridge and the spacing between the two surfaces. As the velocity of approach is constant the instantaneous spacing, $h(t)$ is known. The amount of mass flow rate to either or both surfaces by capillary and gravitational forces is calculated in the code by $\dot{m} = \rho\tilde{v}\phi/J$. Where $\tilde{v}$ is the contravariant velocity $\tilde{v} = u\eta_x + v\eta_y + w\eta_z$ with η's and J being the metrics and Jacobian of the coordinate transformations, respectively. The remaining mass divided by the liquid density will yield the instantaneous volume of the liquid bridge, V_{Liq}. Then, Eq. A1 can be solved as summarized

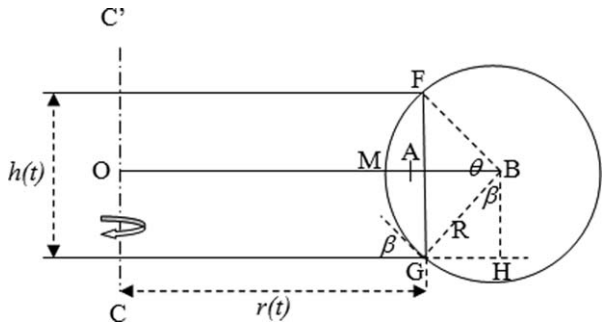

in Eq. 2 in the text, to find the instantaneous radius of the footprint.

The spread is assumed to stop when the height becomes less than a threshold where at that time the radius stays constant (no further motion due to contact, but still a very thin liquid bridge exists) and the height will be reduced according Eq. A1, as the absorption into the porous media causes the remainder of the fluid to be absorbed further bringing the final value of $h(t)$ to zero. This is how Eq. 3 is derived.

Manuscript received Feb. 6, 2013, revision received Sept. 19, 2013, and final revision received Jan. 23, 2014.